CrossMark

ORIGINAL PAPER

Characterization of tropical precipitation using drop size distribution and rain rate-radar reflectivity relation

Saurabh Das[1] · **Animesh Maitra**[2]

Abstract Characterization of precipitation is important for proper interpretation of rain information from remotely sensed data. Rain attenuation and radar reflectivity (Z) depend directly on the drop size distribution (DSD). The relation between radar reflectivity/rain attenuation and rain rate (R) varies widely depending upon the origin, topography, and drop evolution mechanism and needs further understanding of the precipitation characteristics. The present work utilizes 2 years of concurrent measurements of DSD using a ground-based disdrometer at five diverse climatic conditions in Indian subcontinent and explores the possibility of rain classification based on microphysical characteristics of precipitation. It is observed that both gamma and lognormal distributions are performing almost similar for Indian region with a marginally better performance by one model than other depending upon the locations. It has also been found that shape-slope relationship of gamma distribution can be a good indicator of rain type. The Z-R relation, $Z = AR^b$, is found to vary widely for different precipitation systems, with convective rain that has higher values of A than the stratiform rain for two locations, whereas the reverse is observed for the rest of the three locations. Further, the results indicate that the majority of rainfall (>50%) in Indian region is due to the convective rain although the occurrence time of convective rain is low (<10%).

✉ Saurabh Das
das.saurabh01@gmail.com

Animesh Maitra
animesh.maitra@gmail.com

1 Centre for Soft Computing Research, Indian Statistical Institute, 203 Barrackpore Trunk Road, Kolkata, WB 700108, India

2 Institute of Radio Physics and Electronics, University of Calcutta, Kolkata, India

1 Introduction

Quantitative precipitation estimation (QPE) is an important objective for radar meteorology and space-borne remote sensing, which requires an in-depth understanding of the precipitation structures. On the other hand, knowledge of precipitation is important for high-frequency band communications. The interest is renewed on the subject recently mainly due to the requirement of ground validation and interpretation of satellite-based measurements, especially in view of Dual Frequency Radar (DPR) onboard Global Precipitation Mission (GPM) satellite. The performance of weather radar is also relaid on the accurate modeling of the radar reflectivity and rain rate, which is very critical for real-time flood warning systems. It also got the attention because of recent interest to go beyond 10 GHz frequencies for satellite communications where rain is the primary cause of impairments (Asen 2002; Das et al. 2010a, b; Obiyemi et al. 2016).

The rain is usually characterized in terms of drop size distribution (DSD). Due to the complex nature of drop formation either by condensation of small droplets or from the melting layer, it is expected to vary within a rain rate for a particular location (Tokay and Short 1996). The broader spectrum of DSD variation leads to different attenuation and radar reflectivity values for a specific rain rate value. DSD also varies widely for different locations and even in storm to storm. Many works have been done to characterize the DSD in both temperate and tropical locations (Bringi et al. 2012; Thurai et al. 2010; Caracciolo et al. 2008; Kozu et al. 2006; Rao et al. 2002; Prat and Barros 2010; Campos et al. 2006); yet, this is one of the areas which still need further data for better understanding of the process.

The DSD is normally modeled in two-parameter Marshall and Palmer (1948) or exponential models, which are not always good approximations in the case of tropical rainfall (Timothy et al. 2002; Das et al. 2010a, b; Maitra 2000).

Springer

Consequently, three-parameter gamma and lognormal models are used to describe the rain DSD (Timothy et al. 2002; Kozu et al. 2006; Bringi et al. 2012). As the cloud microphysics plays an important part in the shape of DSD (Tokay and Short 1996), it is expected to vary for different rain conditions. Also, the presence of aerosols and pollutions is the important controlling factor of the shape of DSD. Besides, tropical rain is dominated by the convective type of rain, and thus, local topography is playing a crucial role in determining the shape of DSD.

Rain attenuation and radar reflectivity not only depend on the rain rate but also depend on the type of rain (Rao et al. 2002; Das et al. 2010a, b; Thurai et al. 2010). In addition to the varied DSD, different types of rain are associated with the different vertical and horizontal rain structure, which in turn attenuate and scattered back signal differently. The understanding and classification of precipitation process are thus very crucial for the scientific community to address these challenging problems.

The classifications of precipitation can be made based on the vertical wind velocity and fall velocity of hydrometeors (Houze 1993). In the stratiform rain, vertical air motion is small compared to the fall velocity of hydrometeors and provides a suitable environment for melting layer formation. Unfortunately, conventional weather radars and space-borne radars like Precipitation Radar (PR) onboard Tropical Rainfall Measuring Mission (TRMM) satellite or DPR do not have the capability to measure the speed of the air or hydrometeor. However, the melting layer can cause high reflectivity due to the change in dielectric property and can be detected as the bright band in radar reflectivity profile. The occurrence of a bright band can be treated as a signature of stratiform rain (Fabry and Zawadzki 1995). Rain classification based on the cloud structure is also proposed by many researchers (Gamache and Houze 1982; Churchill and Houze 1984).

The use of radar is not always possible for all locations. It is thus always useful to discriminate the rain by ground-based rain rate and drop size measurement only, as these are easily measurable quantity. These kinds of approaches use the relationship of rain with radar reflectivity factor to discriminate between convective and stratiform (Fujiwara 1965; Joss and Waldvogel 1969). A threshold value of 0.5 mm per 5 min is used by Johnson and Hamilton (1988) for rain classification, where the rain above this threshold is assumed to be of the convective type. Similarly, Gamache and Houze (1982) propose a threshold reflectivity factor of 38 dBZ for rain classification, where below the thresholds are classified as the stratiform case and vice versa.

Waldvogel (1974) used a rain classification scheme based on the N0 jump of fitted gamma distribution to rain DSD. Temporal variation of gamma parameter is also used by Tokay and Short (1996) for rain classification in tropical Ocean Global Atmosphere Experiment (TOGA-COARE).

They also reported the characteristic difference of DSD between the two types of rain. Classification based on DSD has an added advantage that it provides a further understanding of the precipitation process as well. It gives also an insight into the microphysical behavior of cloud as the variation of DSD occurs due to different rain forming process (Caracciolo et al. 2008).

However, the rain classification studies are mostly concentrated on two types of rain, and very few studies take care of the shallow convective or heavy stratiform cases, which occurs at transitions (Williams et al. 1995; Caracciolo et al. 2008). This transition rain can cover a significant portion of total accumulated rainfall (Rao et al. 2002). Further, rain classification schemes have been applied mainly to temperate regions (Waldvogel 1974; Ulbrich 1983; Zawadski et al. 1994), and over tropical oceans (Tokay and Short 1996; Testud et al. 2001), little work has been done over tropical landmass (Rao et al. 2002). The situation is more critical as the DSD characteristic changes with locations and measurement from different climatic conditions are essential for satellite-based rainfall estimation.

One of other aspects of the rain classification is to identify suitable Z-R relationship for radar meteorology and space applications. The applicability of radar depends on how suitably Z-R relationship has been derived. It has been usually done by assuming a power law relationship between rainfall intensity (R) and radar reflectivity factor (Z), $Z = AR^b$, where A and b are constants. Various values of A and b are reported for different regions after the initial works carried by Marshall and Palmer in 1948.

The present study reports on the tropical precipitation characteristics in terms of DSD and Z-R relationship for five locations in Indian subcontinent using ground-based disdrometer measurements. This is one of the most comprehensive ground-based measurements of precipitation in terms of DSD from different climatic regions in India. Suitability of DSD modeling in terms of lognormal and gamma distribution is assessed for these locations. The behavior of different modeling parameters and their possible use for rain classification are also studied. These analyses also aimed to identify the suitable Z-R relationship for different rain types for these regions.

2 Description of the instrument and data collection

Data used for the present study are obtained from five diverse geographic locations spread across tropical India—Ahmedabad (AHM) (23°04′, 72°38′), Hassan (HAS) (13°, 76°09′), Shillong (SHL) (25°34′, 91°53′), Kharagpur (KGP) (22°32′, 88°20′), and Trivandrum (TVM) (08°29′, 76°57′) as shown in Fig. 1. Except for Shillong, all other locations are in plane areas. Shillong is located in the north-eastern hilly

Fig. 1 Locations of the measurement sites
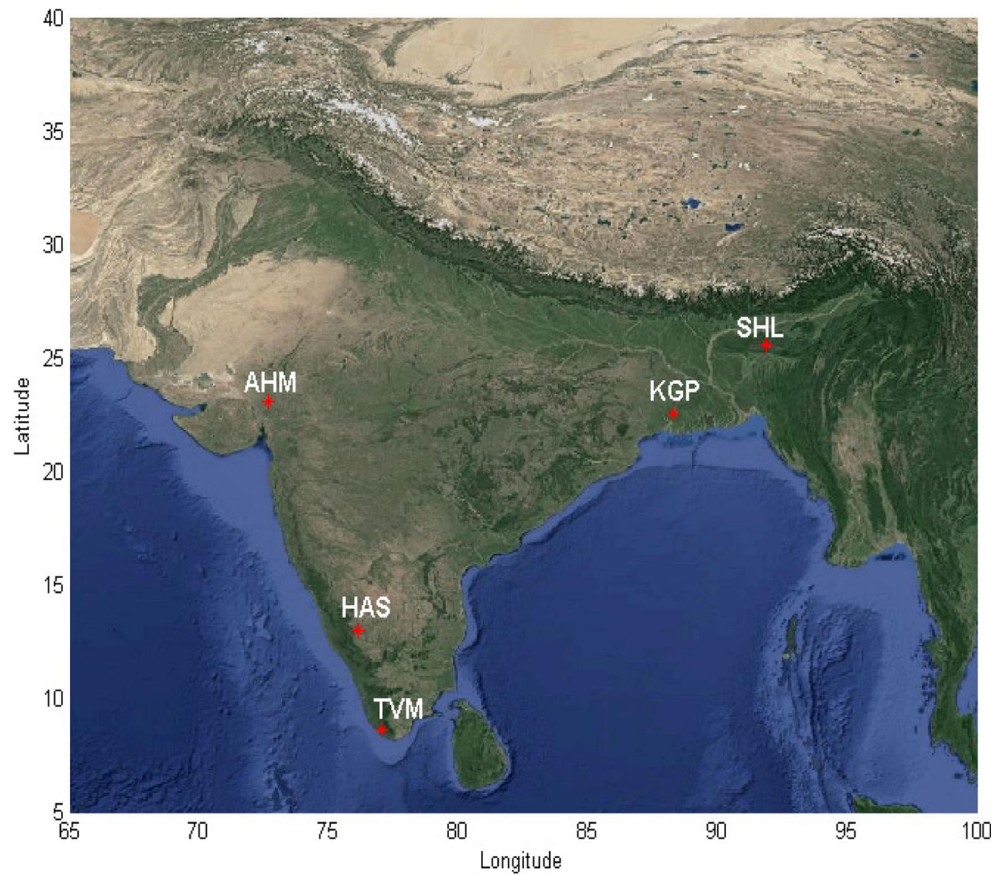
region of Himalayas. Hassan is situated in southern India. Kharagpur, a coastal region, is located in the eastern part of India. Trivandrum is also a coastal area in southern India. Ahmedabad is situated in the western region of India with rainfall occurring mainly in monsoon season. The data has been collected at these locations under "Ka-band propagation Experiment" by Indian Space Research Organization (ISRO) during 2006–2007. This is one of the most exhaustive data set of rain DSD over Indian region considering the varied rain climatology of these places.

In India, four seasons are prevalent. Most of the rain occurs over India during monsoon season (June–Sept.) due to South-West monsoon circulation. The monsoon wind carries the moisture from the ocean to the land surfaces and is the primary source of rainfall in India. Rain during the post-monsoon (Oct.–Nov.) season occurs by the retreated monsoon wind due to the presence of Himalayas. In general, rain is relatively scarce at most of the places due to North-East monsoon circulation where the wind blows from land surface to the ocean and significant rain occurs only over the Indian peninsular region and some part of north-east India. During pre-monsoon (March–May) and winter (Dec.–Feb.) season, rainfall over India is mostly due to local convective activities. Winter season is the driest among all the seasons over India.

In all the locations, drop size measurement has been made using disdrometer (Disdromet RD-80). The disdrometer is an impact type drop size counter. The stability and performance of such instruments are widely reported and are extensively used by research community (Tokay and Short 1996; Das et al. 2010a, b). The drop size distribution has been obtained in 20-drop size classes (0.3–5 mm) by disdrometer. Once the drop size distributions are known, rain rate and radar reflectivity factor can be calculated as follows:

$$R = \frac{\pi}{6} * \frac{3.6}{10^3} * \frac{1}{A.t} \sum_{i=1}^{20} \left(n_i . D_i^3 \right)$$

and

$$Z = \frac{1}{At} \sum_{i=1}^{20} \frac{n_i}{V(D_i)} D_i^6$$

where

A = total area of observation
t = Integration time
n_i = number of drops for size class i
D_i = mean diameter of size class i
$V(D_i)$ = fall velocity of a drop with diameter D_i

The disdrometer measures the momentum of falling rain drops. Assuming that drops are falling with terminal velocity, the momentum of the drops can be related to equivalent spherical rain drop diameter (Gunn and Kinzer 1949). The disdrometer was configured for an integration time of 30 s.

Major errors in disdrometer measurements are due to mainly three reasons: (1) wind, (2) acoustic noises, and (3) insensitivity of disdrometer surface after splashing of a large drop (dead time). Proper installation is assured to minimize the error due to wind and acoustic noise. The instrument is kept at the rooftops of the buildings for different locations. The position was chosen away from any obstructing structure nearby to avoid artificial wind turbulence and other acoustic noise sources. Dead time correction for the insensitivity due to ringing of the larger drop is not applied as it does not provide very different results for moderate rain rate (Asen 2002) and error in Z-R relationship is less than 3% (Tokay and Short 1996). The instrument was connected to a data logger for continuous logging of the data.

The instruments are tried to kept operational during all the seasons for most of the locations. Due to logistic constraints, only monsoon period rain data are measured at AHM. For SHL and HAS, winter rain is not measured due to the same reason. The downtime of the instruments during the measurement period is less than 10% for the rest of the seasons and locations. Table 1 shows the total and seasonal rain accumulation during the observation period. It can be seen that HAS received lowest rainfall among all these locations since it is located in the rain shadow region of Western Ghats. The majority of rainfall occurs during South-West monsoon at all the places. TVM, HAS, and SHL also receive substantial rain during the post-monsoon season (North-East monsoon).

The quality of the data is checked regularly using collocated tipping bucket rain gauge measurements of rain rate during the measurement period (Das et al. 2010a, b; Maitra et al. 2009). The rain gauge (KWS032, Komoline India Pvt. Ltd.) is a tipping bucket type with a collection area of 200 cm^2. It is connected with a GPS receiver to measure the time instant of each tip which needs 0.25 ml of rain accumulation before each tip. The instrument has a minimum temporal resolution of 1 s.

3 Data reduction and modeling

DSD characteristics vary for different reasons. Wind motion from oceans or land can influence the DSD characteristics, particularly for locations in coastal regions (Tenório et al.

2012). However, the significant influence on DSD comes primarily through the change in rain types. Since the wind directions change for different seasons, it can be treated as an indicator of the land-ocean or ocean-land transition. In this study, the seasonal variability of rain microstructure is also investigated to see if there is any significant effect of wind motion direction on rain DSDs of different types.

The rain characterization in the present work is performed primarily based on the DSD features of these locations. For this purpose, the DSD needed to be modeled in some mathematical forms. Three-parameter lognormal and gamma distributions are found in the literature to be more suitable in describing DSD, especially for tropical regions. Hence, we have fitted the observed DSD with these two distributions. The method of moment technique has been used for calculating the parameters of the models. The fitting has been performed for each instant, and the respective parameters are stored in a matrix with disdrometer-measured rain rate values. The data have also been grouped in different rain rate bins and averaged over the said measurement period. The average DSD is then fitted with these two distributions. These provide a good understanding of how the different models represent the actual DSD.

Lognormal distribution function is given as follows (Timothy et al. 2002),

$$N\,(D)\; =\; \frac{N_T}{\sigma D\sqrt{2\pi}}\, \exp\left[\frac{-0.5(\ln(D)-\mu)^2}{\sigma^2}\right]$$

where, $N(D)$ is the number density (in m^{-3}/mm^1), N_T is the total number of drops, D is the drop diameter (in mm), σ is the standard deviation, and μ is the mean of $\ln(D)$. N_T, σ, and μ are the rain rate-dependent variables.

Assuming the range of drop diameter from 0 to ∞, the ith moment of this distribution (X_i) can be expressed as

$$X_i = N_T\exp\left\{i\mu + \frac{1}{2}\left(i^2\sigma^2\right)\right\}$$

In the present case, 3rd, 4th, and 6th moments are used for estimation of model parameters by simultaneously solving three equations developed from above formulation. Though other moments can also be used for such purpose, these

Rain accumulation	Ahmedabad (mm)	Trivandrum (mm)	Shillong (mm)	Kharagpur (mm)	Hassan (mm)
Total	1661	3138	3774	2517	1304
Pre-monsoon	–	450	788	122	92
Monsoon	1661	1727	2404	2236	829
Post-monsoon	–	861	582	73	383
Winter	–	100	–	86	–

Table 1 Rain accumulation during the measurement period

"–" indicates absence of measurement

moments are chosen for estimation of model parameters as they are related to rain rate, attenuation, and radar reflectivity, respectively. Mathematical relationship of the model parameters thus obtained with these moments are given as follows

$$N_T = \exp\left[\frac{1}{3}(24L_3 - 27L_4 + 6L_6)\right]$$

$$\mu = \frac{1}{3}(-10L_3 + 13.5L_4 - 3.5L_6)$$

$$\sigma^2 = \frac{1}{3}(2L_3 - 3L_4 + L_6)$$

where L_3, L_4, and L_6 are the natural logarithms of 3rd, 4th, and 6th moments, respectively.

The gamma model parameters are also estimated similarly. The gamma distribution is given by

$$N(D) = N_0 D^m e^{-\Lambda D}$$

Distribution parameters m, Λ, and N_0 signify the shape, scaling, and amplitude, respectively. These parameters are also evaluated by the method of moment technique (Kozu and Nakamura 1991). The final relations obtained between gamma model parameters and the moments of the distribution are as follows:

$$m = \frac{11G - 8 + \sqrt{G(G+8)}}{2(1-G)}$$

$$G = \frac{M_4^3}{M_3^2 M_6}$$

$$\Lambda = \frac{m+4}{dm}$$

$$N_0 = \frac{\Lambda^{(m+4)} M_3}{\Gamma(m+4)}$$

$$dm = \frac{M_4}{M_3}$$

where M_3, M_4, and M_6 are the moments of the distribution.

The modeled lognormal and gamma distribution parameters estimated as above have been tested against each actual measured DSD. The testing of the models is based on measured rain rate values. Two criterion has been chosen for testing the models with original measurement—root mean square error (RMSE) and average probability ratio (APR). RMSE is given by

$$\text{RMSE} = \sqrt{\frac{1}{N}\sum_{i=1}^{N}\left(V_i^{est} - V_i^{mes}\right)^2}$$

where V_i^{est} is the estimated value from model at i^{th} instance and V_i^{mes} is the actual measurement of that instant. N is the total number of measurement instances.

APR is given by

$$APR = \frac{1}{M}\sum_{j=1}^{M}\frac{P_j^{est}}{P_j^{mes}}$$

where P_j^{est} and P_j^{mes} are the cumulative probability values at sampling point j. The measured quantity is equally divided in to 100 bins (M) and cumulative probability is obtained.

The modeled parameters are then studied and rain classification is attempted based on these parameters. The Z-R relations for each location and for different rain types are then estimated.

4 Results

4.1 Rain drop size distribution and variations of the model parameters

To compare the changes in DSD characteristics among different locations, average DSD combining all rain rates is shown in Fig. 2. It can be seen that the significant variations of number concentrations are observed among different locations for the medium size drops. The variations of number concentrations are relatively less at both the ends. Drop concentrations are found to be maximum for KGP and lowest for HAS for medium size drops whereas almost similar drop concentrations for TVM, SHL, and AHM are observed. The DSD for all locations show two peaks, one at less than 1 mm drop size and the other between 1 and 2 mm drop size. The position of the peak drop concentration depends upon the rain drop evolution mechanism throughout the height range. Usually, the peak gets right shifted with an increase in rain rates and in convective rain type. Since in present case, averaging was done comprising all types of rain as well as rain rates, two distinct peaks (though the 2nd one is of much less magnitude) are observed.

In Fig. 3, the seasonal variations of average DSD for different locations are shown. AHM is not shown in this figure as
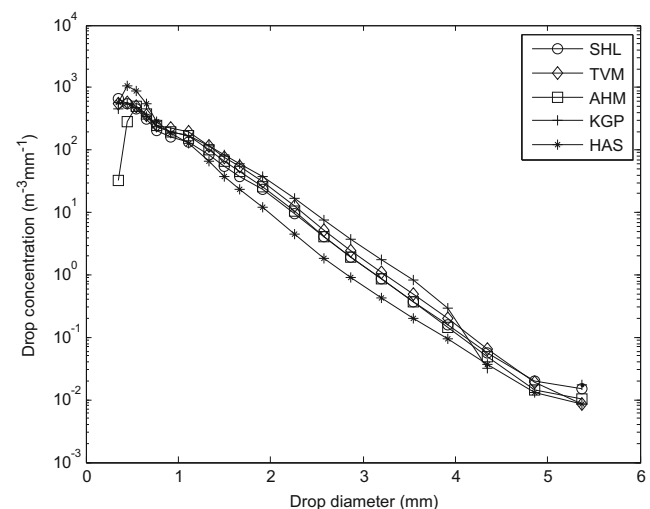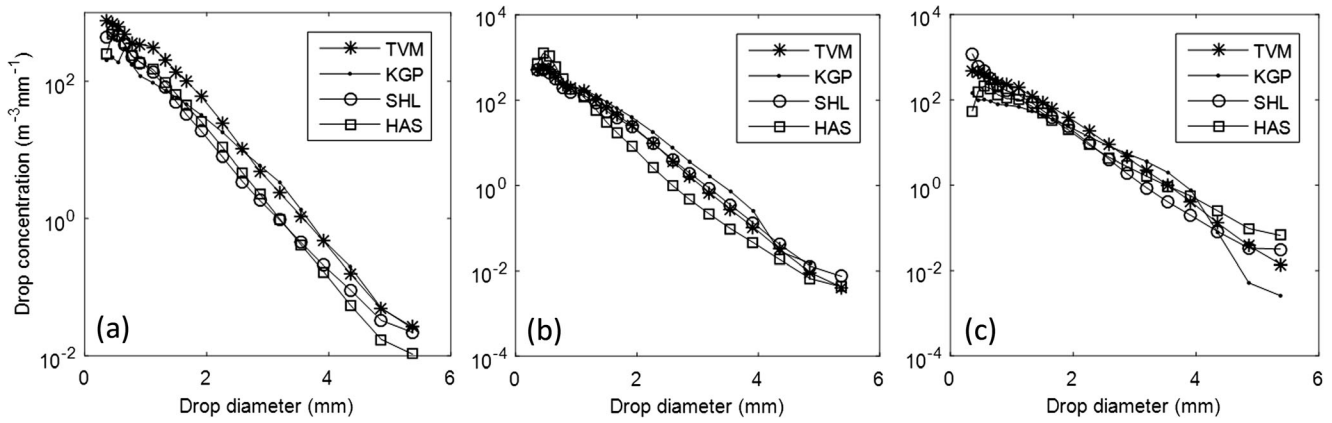

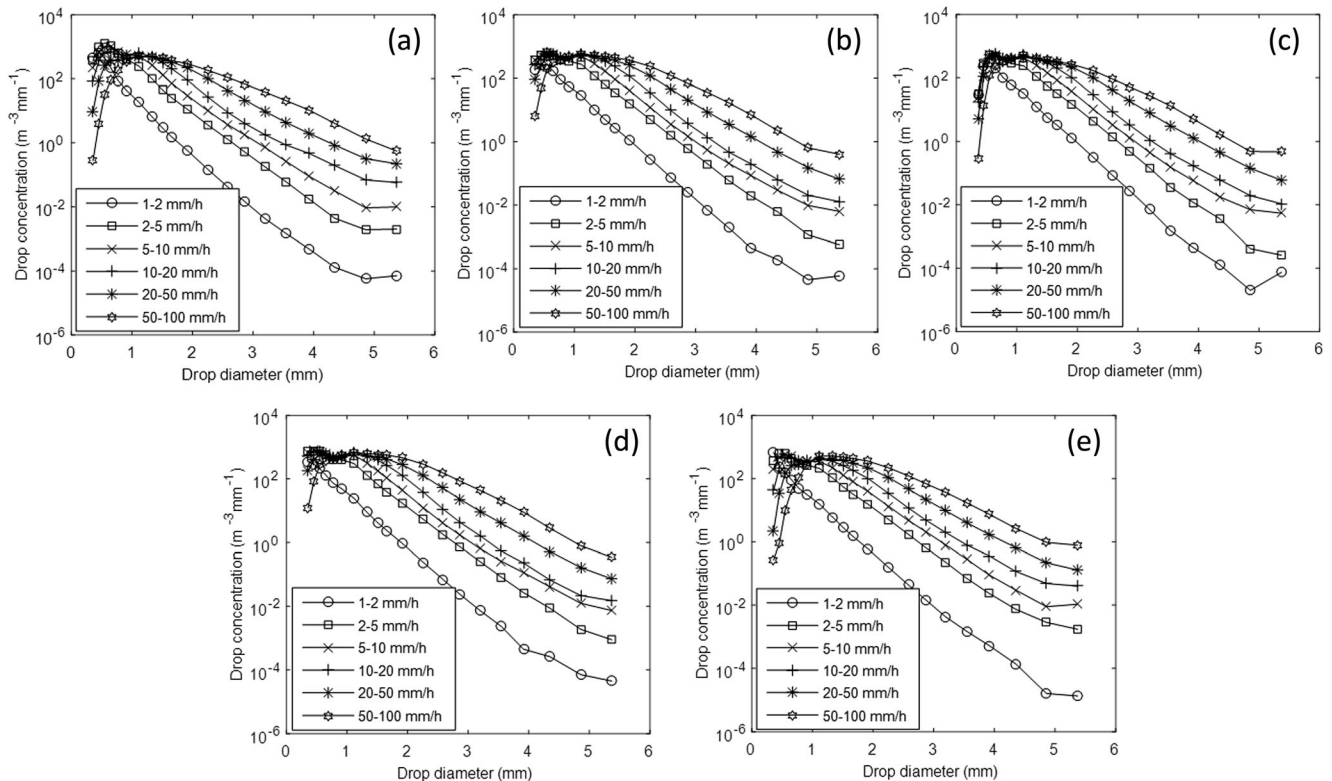**Fig. 2** Average drop size distribution of different locations

Fig. 3 Seasonal variations of the average drop size distributions of different locations for **a** pre-monsoon, **b** monsoon, and **c** post-monsoon

only monsoon rain is measured at Ahmedabad. One can note that the behavior of seasonal DSDs varies for different locations. In pre-monsoon season, SHL and HAS show similar DSD variations whereas, in monsoon, SHL and TVM show similar DSD characteristics. The variations of average DSD for different seasons are due to changes in the proportion of different types of rain in the total rain as well as different rain formation process.

It is, therefore, more informative to study the DSD separately either for different rain rate ranges or for different rain types. As rain rate information can be more accurately measured by this ground-based instrument than the rain type information, DSD characteristics for different rain rate ranges are presented next.

In Fig. 4, average rain DSD for different rain rate ranges for all the study regions is shown. It can be seen that there are differences in the drop concentrations at different drop sizes among the study locations, but the nature of the curves are similar for all locations. It can be seen that the DSD becomes flatter as the rain rate increases. The peak of the distribution is also seen to shift towards large drop sizes with increase in rain rate and is a general feature of these locations. Usually, convective rain is associated with more number of large rain drops and high rain rates. Accordingly, the drop concentrations of the large drops increase with an increase in rain rate.

To identify the most suitable model representing the DSD characteristics of the study locations, DSDs of each location are

Fig. 4 Drop size distributions for different rain rate ranges for **a** HAS, **b** KGP, **c** AHM, **d** TVM, and **e** SHL

Fig. 5 Average and modeled DSD over SHL for **a** 2–3 mm/h and **b** 20–25 mm/h. *Vertical lines* indicate the standard deviation value
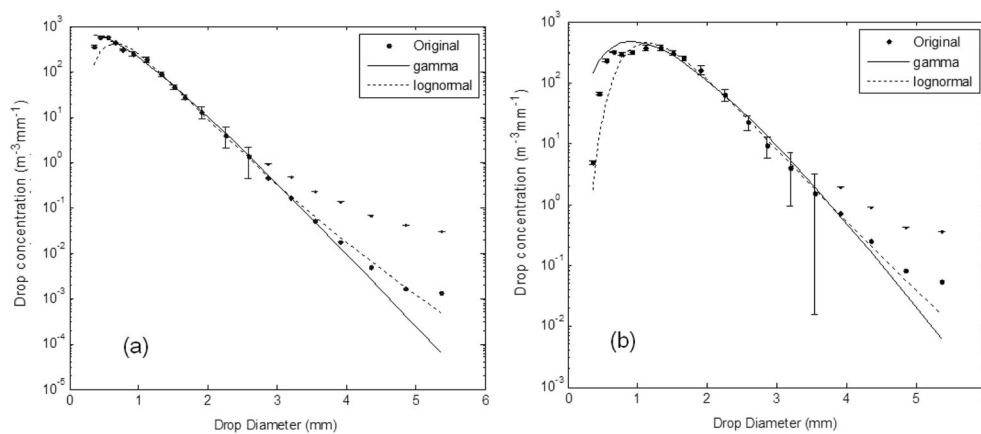
then fitted with gamma and lognormal functions, and model parameters are estimated as discussed in Sect. 3. In Fig. 5a, average DSD of SHL and corresponding distribution models is shown as a representative figure for the rain rate range 2–3 mm/h. In Fig. 5b, similar results are shown for rain rate range 20–25 mm/h. It shows that at the lower end of the DSD, gamma distribution tends to over-estimate while lognormal distributions under-estimate. At the higher end of DSD, the gamma model under-estimate the drop concentration while lognormal over-estimate. However, the performances of both these models are equally good at the intermediate drop sizes. This type of behavior is observed for other locations also. The gamma distribution is found to be better fitted in low rain rates than lognormal distribution.

In Table 2, RMSE and APR values of rain rate calculated from DSD and that from both the gamma and lognormal models are given. Instead of using the average DSD for performance evaluation, we fit both the models to instantaneous DSD. The rain rate is then calculated from both measured DSD and modeled DSD. The RMSE and APR are then estimated based on the whole data set.

One can note that the lognormal model performed better than gamma model for KGP and AHM on the basis of both RMSE and APR, whereas gamma model is superior to lognormal model for SHL. TVM and HAS show low RMSE value for lognormal but low APR value in case of gamma model. Nevertheless, the study indicates that both of these models can be used for rain rate estimation with low error probability. The lognormal model is used to estimate rain attenuation characteristics over different regions in an earlier study (Das et al. 2010a, b). Here, for the present study, the rain classification is attempted using gamma model.

Examples of the behavior of the gamma model parameters are shown in Fig. 6 for SHL. Other locations also indicate the similar behavior of the model parameters and not shown here. One can note that the distribution of all these parameters is significantly broad in low rain rates. A similar observation can also be made with the lognormal model. This indicates the presence of varied DSD in low rain rates, whereas the DSD shapes at high rain rates are more stable than the low rain counterpart. Further, total numbers of drops in low rain rate are often inadequate to be represented accurately by any models. This also leads to wide variations in model parameters in low rain condition. In our study, since we do not use any restriction on the number of rain drops, the model may not be very accurate at low rain rates. Fortunately, although the occurrence of high rain rates is less frequent, the amount of rainfall is significant.

4.2 Rain classifications

The rain classification is attempted by different researchers in different ways as already mentioned in the introduction. It is often assumed that the rain rate value 2 mm/h is usually stratiform type and above 10 mm/h is the convective type (Caracciolo et al. 2008). Rain classification is also reportedly done by using radar reflectivity (Gamache and Houze 1982), in which above 38 dB is assigned to the convective type and below 38 dB is assumed to be the stratiform type. In our approach, we use a mixture of both the conditions as demonstrated with the data from Italy by Caracciolo et al. (2008). The rain has been classified into groups by rain rate and radar reflectivity factor.

Table 2 Performance of lognormal and gamma model

| Criterion	Model	Kharagpur	Ahmedabad	Trivandrum	Shillong	Hassan
RMSE in rain rate	Gamma	2.59	2.1997	2.1138	1.0862	0.91956
	Lognormal	1.3385	0.78731	1.6432	1.4481	0.6654
APR in rain rate	Gamma	1.0025	1.0014	1.0005	1.0003	0.99925
	Lognormal	1.0012	1.0001	1.0007	1.0013	0.99996
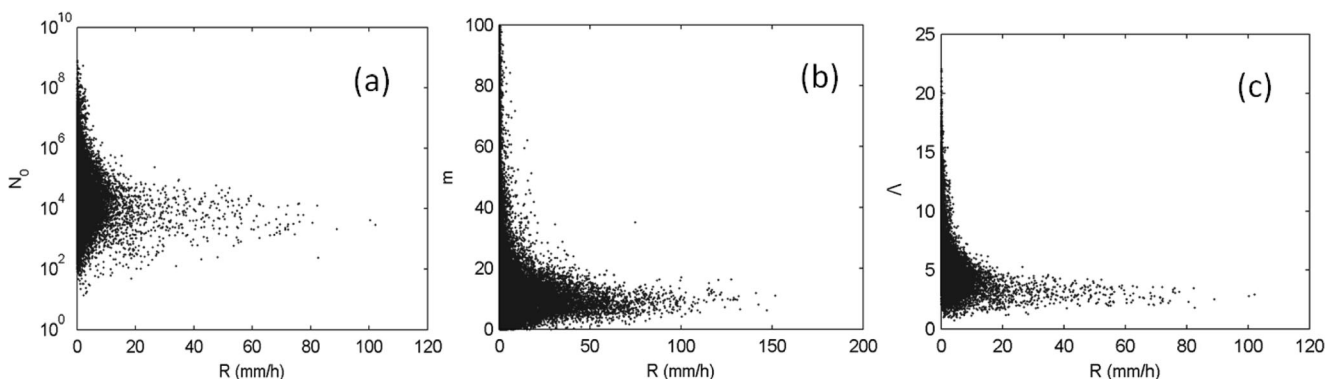
Fig. 6 Variations of the gamma model parameters with rain rate at SHL

a. $R < 10$ mm/h and $Z < 38$ dB implies strong stratiform.
b. $R > 10$ mm/h and $Z > 38$ dB implies strong convection
c. $R > 10$ mm/h and $Z < 38$ dB (heavy stratiform) or $R < 10$ mm/h and $Z > 38$ dB (shallow convective) indicates mixed rain type.

The behaviors of gamma parameters are then studied for different rain types. The variations of peak drop diameter and mean volume diameter for different rain types are also investigated. The peak diameter (D_p) can be estimated as $D_p = m/\Lambda$, whereas the mean volume diameter (d_m) is estimated by the 3rd and 4th moment of the DSD. D_p indicates the modal peak and d_m indicates the mass weighted mean diameter. It is found that the m vs Λ of gamma distribution provides a good clustering of different type of rain which in turns allows identifying a suitable curve of m-Λ between these two types. These are shown in Fig. 7.

One can note that the low Λ values correspond to convective rain for same m values and are due to large numbers of smaller drops in the stratiform rain than the convective rain. The convective cases have significant numbers of larger drops making a concave nature of the DSD. This means that the for fixed Λ value, shape factor m will be large (Caracciolo et al. 2008). This procedure has been repeated over all the locations, and the discrimination line has been obtained in the form of $C_1 * \Lambda - m = C_2$. The values of C_1 and C_2 are found to vary in a narrow range for all these locations, with C_2 varying from 3.9 to 4.2 and C_1 varying between 1.3 and 1.6. Similar discrimination line as $1.635\Lambda - m = 2$ is reported by Caracciolo et al.
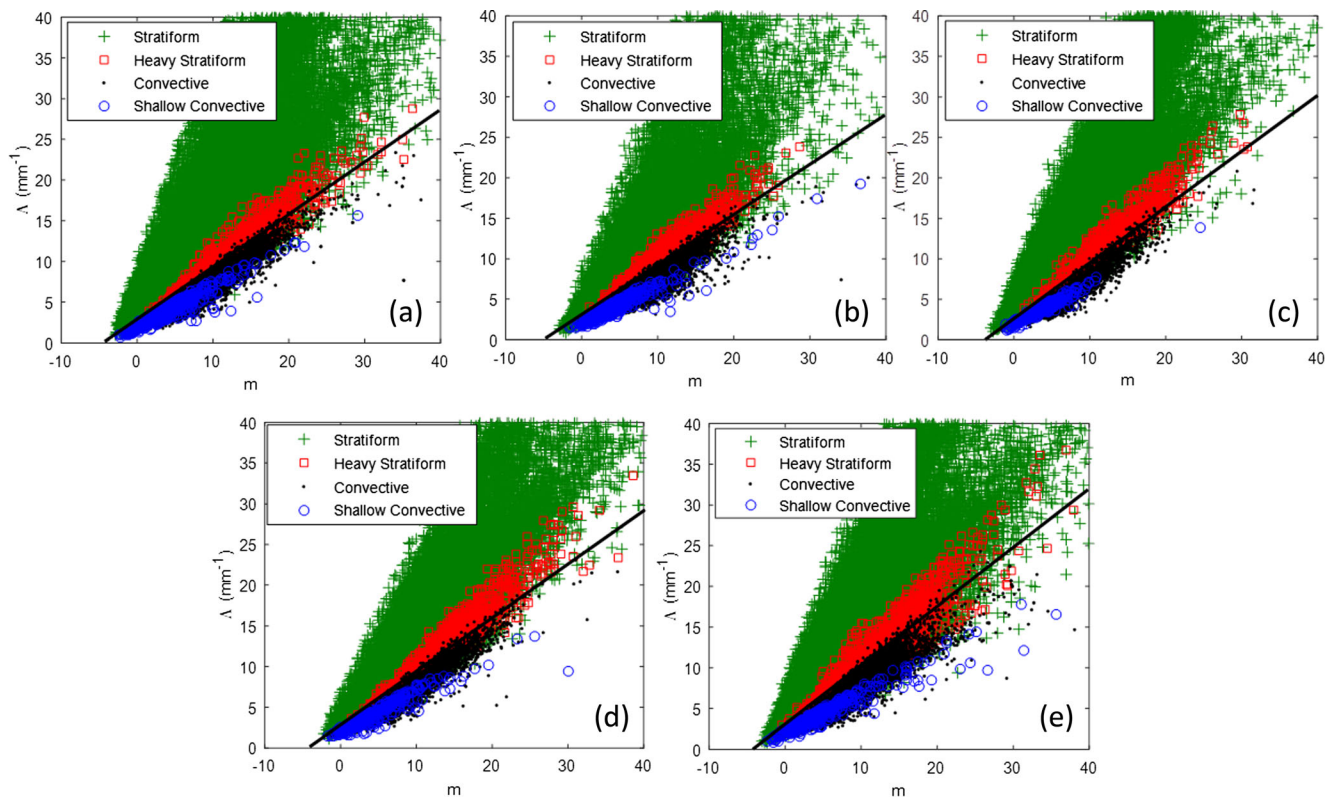
Fig. 7 Λ-m relation for different rain types for **a** HAS, **b** KGP, **c** AHM, **d** TVM, and **e** SHL
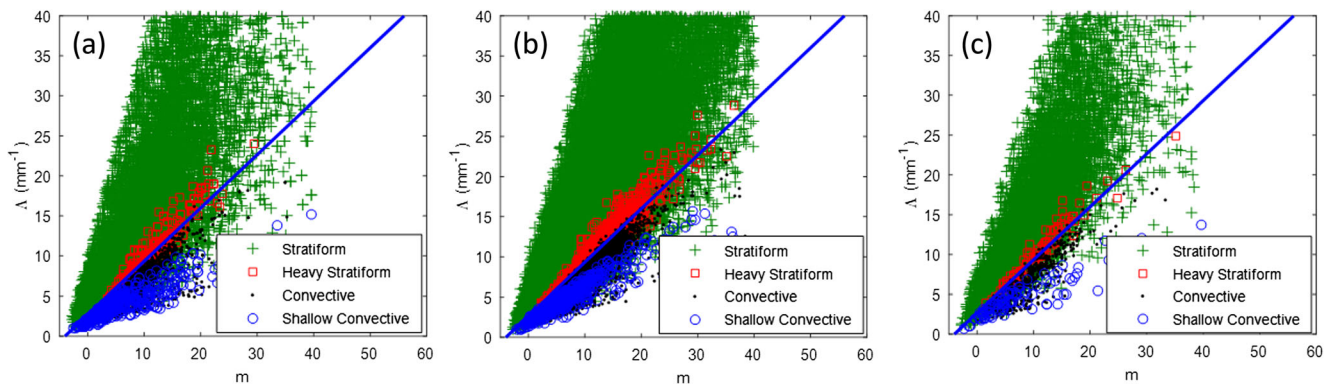
Fig. 8 Seasonal variations of Λ-m relation for different rain types for **a** pre-monsoon, **b** monsoon, and **c** post-monsoon

(2008) from Italy. The mixed rain consisting of shallow convective and heavy stratiform rain features is intermediate to convective and stratiform rain.

In Fig. 8, the seasonal variations of m-Λ relation are shown for the coastal region of TVM. It is to be noted here that TVM received significant rain during both monsoon and post-monsoon period. During monsoon, a majority of the wind is from South-West direction (ocean to land) whereas during post-monsoon, it is from North-East direction (land to the ocean). Hence, Fig. 8 can also highlight the effect of land-ocean (or ocean-land) transition of the precipitating system on rain microstructure. It can be seen here that the demarcation line between stratiform and convective are similar for all the

seasons and m-Λ relation changes significantly only for different rain types. However, m-Λ relation of individual points shows some changes for different seasons. The other locations also indicate similar seasonal characteristics and do not provide any further insight, hence not shown here. The results indicate that the rain classification line is invariant for different seasons and/or wind motion direction, but the rain microstructure changes to some extent for different seasons.

The variations of gamma parameter N_0 is further studied with mean volume diameter. In Fig. 9, the scatter plot of N_0 with mean volume diameter is shown for different locations. It is observed that higher N_0 is associated with convective rain than the stratiform rain for the same mean volume diameter.
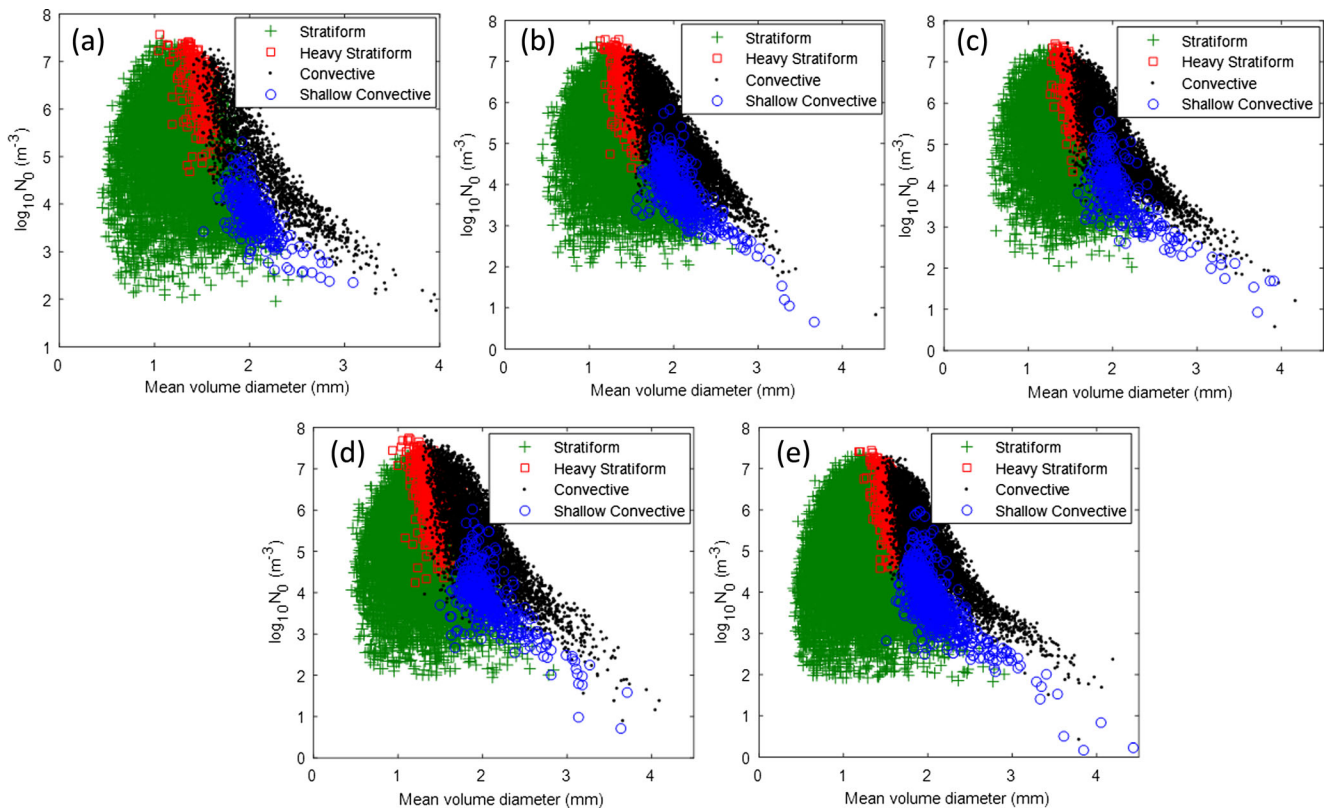
Fig. 9 Variations of N_0 with mean volume diameter for **a** HAS, **b** KGP, **c** AHM, **d** TVM, and **e** SHL

This again supports the fact the convective rain is composed of more number of large drops than the stratiform case. This is also a general feature which is observed for all the locations and also reported by many researchers from various locations. The mixed rain consisting of shallow convective and heavy stratiform rain features is intermediate to convective and stratiform rain.

### 4.3 Z-R relation and contribution of different rain type in total rainfall

The relationship between radar reflectivity and rain rate is often used for rain classification (Fujiwara 1965; Hazenberg et al. 2011). On the other hand, the retrieval of rain rate from radar reflectivity in weather radar often uses separate relations for stratiform and convective rain. The accuracy of the retrieval is thus closely associated with the accuracy of which these parameters of the equation are derived. In general, a power law equation is used to model these parameters, i.e., $Z = AR^b$ where Z in mm^6/m^3 and R in mm/h. The parameters A and b are dependent on various factors including rain type, location, topography, cloud structure etc. In general, a high A value corresponds to the convective case where as a small A signifies stratiform rain; however, reverse case is also reported (Rao et al. 2002).

The values of A and b are obtained by linear regression of log(Z) with R for the present study. The obtained values of the coefficients are compared in Fig. 10 separately for both convective and stratiform rain with the reported values from other locations. It is to be noted here that the whole data set is utilized in deriving the Z-R relation at these places. There could be strong seasonal changes of Z-R relation if one analyze the data without rain type classification (Das and Ghosh

Fig. 10 Variations of A and b parameters for different locations. The values from other researchers are represented as SR—Sivaramakrishnan (1961); S—Short et al. (1990); NR—Narayan Rao et al. (2002); TS—Tokay and Short (1996); F—Fujiwara (1965); SS—Sekhonan and Sekhon and Srivastava (1971); MP—Marshall and Palmer (1948); N—Narayana Rao et al. (1999)

2016; Tenório et al. 2012), though, as pointed out in previous section, the seasonal changes in rain microstructure for same rain type are less significant than for different rain types.

We can note that high A values are obtained for convective cases in SHL and TVM, whereas high A values are associated with stratiform rain in case of HAS, AHM, and KGP. The high A value in stratiform rain is reported by Rao et al. (2002) from Gadanki in India, a nearby location of HAS. Similar observations are also reported by Tokay and Short (1996) over tropical Ocean which shows a small A value for the convective case. On the other hand, high A values in the convective rain are reported by Fujiwara (1965) and Joss and Waldvogel (1969) and a comparatively low value for stratiform rain in mid-latitude regions (Caracciolo et al. 2008). The dissimilarity among different places of India can be contributed to the spatial change of nature of DSD. It is to be noted here that TVM and SHL received rainfall during both South-West monsoon as well as in North-East Monsoon, whereas in the rest of the places, S-W monsoon is primarily responsible for rain. Further, SHL, being a hilly location, received substantial rainfall due to orographic precipitation. The characteristic difference between NE and SW monsoon is thus could be another important factor affecting the Z-R relation over Indian region (Rao et al. 2002; Kozu et al. 2006). The wide variation of the parameters among other regions also may be due to the fact that different classification mechanism and data set were used.

The rain classification scheme is further used to identify the contribution of different rain type in total rain amount for different locations during different seasons and given in Table 3. It can be seen that although the convective rain occurs for a small percentage of time (~10%), the contribution to accumulated rainfall is more than 50% for all the locations. The transition rain is also found to contribute ~20% of the total rain accumulation for all the locations. Similar results are also obtained by Rao et al. (2002).
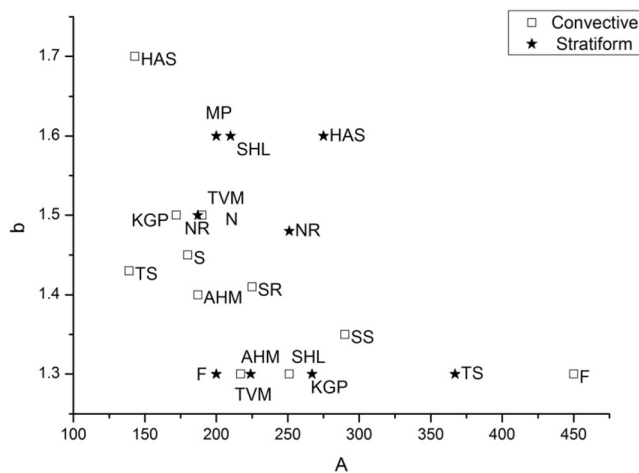
5 Conclusions

Rain characteristic are an important factor for both space-based and ground-based radar meteorology as well as in modeling of high-frequency signal propagation. The drop size distribution is the fundamental quantity which is usually used to model the precipitation. In this paper, the features of tropical rain received at five diverse climatic conditions in Indian region are presented. This is one of the comprehensive simultaneous ground-based measurements of rain DSD over this region.

The modeling of the DSD is attempted using gamma and lognormal form. The large drops are found to be overestimated by lognormal whereas gamma tends to underestimate the large drops. The reverse picture is observed in the case of small drops. However, the overall results indicate

Table 3 Percentage contribution of different rain types on total rain

Location	Convective rain time (%)	Stratiform rain time (%)	Mixed rain time (%)	Convective rain amount (%)	Stratiform rain amount (%)	Mixed rain amount (%)
SHL	7	70	23	52	30	18
AHM	8	68	24	56	26	18
TVM	8	67	25	68	15	17
KGP	12	64	24	69	16	15
HAS	8	70	22	58	24	18

the suitability of both the functions in DSD modeling with a marginally improved result for gamma model in SHL whereas lognormal perform slightly better in the case of AHM and KGP.

The gamma model parameters m and Λ are further used to classify rain. Clustering of the total number of drops with median volume diameter is also observed for different rain types. This study indicates that the convective rain is composed of large drops whereas small drops are abundant in the stratiform rain. The gamma parameter-based rain classification scheme is found to be invariant under seasonal changes, though some changes in rain microstructure is observed for different seasons. The Z-R relationship has been computed based on these classifications, and it is found that the intercept A is higher for the convective case than the stratiform case in case of SHL and TVM, whereas large A value is obtained in the stratiform rain in case of AHM, KGP, and HAS. The possible reason for such changed characteristics is may be due to the change in monsoon circulation and local topography. In TVM and SHL, both SW and NE monsoon are equally dominant whereas in the rest of the places, only SW monsoon is prominent. However, SHL also received orographic precipitation due to its location on a hilly region. Further investigations on these aspects are needed to ensure the role of different monsoons and orography on Z-R relation and will be a subject matter of future studies. The total contribution of different rain type shows that although convective case occurs for ~10% of the time, the amount of rainfall is almost 50%. The mixed rain types also contribute to ~20% of the total rain at these locations.

References

Asen W (2002) A comparison of rain attenuation and drop size distributions measured in Chilbolton and Singapore. Radio Sci 37(3):1034

Bringi VN, Huang G-J, Munchak SJ, Kummerow CD, Marks DA, Wolff DB (2012) Comparison of drop size distribution parameter (D_0) and rain rate from S-band dual-polarized ground radar, TRMM precipitation radar (PR), and combined PR–TMI: two events from Kwajalein atoll. J Atmos Ocean Technol 29:1603–1616

Campos EF, Zawadzki I, Petitdidier M, Fernández W (2006) Measurement of raindrop size distributions in tropical rain at Costa Rica. J Hydrol 328(1–2):98–109

Caracciolo C, Porcu F, Prodi F (2008) Precipitation classification at mid-latitudes in terms of drop size distribution parameters, adv. In Geoscience 16:11–17

Churchill DD, Houze RA (1984) Development and structure of winter monsoon cloud clusters on winter monsoon cloud clusters on 10 December 1978. Journal of atmospheric science 41:933–960

Das S, Ghosh D (2016) Dependency of rain integral parameters on specific rain drop sizes and its seasonal behaviour. J Atmos Sol Terr Phys 149:15–20

Das S, Maitra A, Shukla AK (2010a) Rain attenuation modeling in the 10-100 GHz frequency using drop size distributions for different climatic zones in tropical India. Progress In Electromagnetics Research B 25:211–224

Das S, Shukla AK, Maitra A (2010b) Investigation of vertical profile of rain microstructure at Ahmedabad in Indian tropical region. Adv Space Res 45(10):1235–1243. doi:10.1016/j.asr.2010.01.001

Fabry F, Zawadzki I (1995) Long-term radar observations of the melting layer of precipitation and their interpretation. J. Atmos.Sci. 52:838–851

Fujiwara M (1965) Rain drop size distribution from individual storms. J Atmos Sci 22:585–591

Gamache JF, Houze RA (1982) Mesoscale air motions associated with tropical sqall line. Mon Weather Rev 110:118–135

Gunn R, Kinzer GD (1949) The terminal velocity of fall for water droplets in stagnant air. J Meteorol 6:243–248. doi:10.1175/1520-0469(1949)006<0243:TTVOFF>2.0.CO;2

Hazenberg P, Yu N, Boudevillain B, Delrieu G, Uijlenhoet R (2011) Scaling of raindrop size distributions and classification of radar reflectivity–rain rate relations in intense Mediterranean precipitation. J Hydrol 402(3–4):179–192

Houze RA (1993) Cloud dynamics. Academic, San Diego

Johnson RH, Hamilton PJ (1988) The relationship of surface features to the precipitation and air flow structure of an intense midlatitude squall line. Mon Weather Rev 116:1444–1472

Joss J, Waldvogel A (1969) Rain drop size distribution and sampling size errors. J Atmos Sci 26:566–569

Kozu T, Nakamura K (1991) Rainfall parameter estimation from dual radar measurements combining reflectivity profile and path-integrated attenuation. J Atmos Ocean Technol 8:259–271

Kozu T, Reddy KK, Mori S, Thurai M, Ong JT, Rao DN, Shimomai D (2006) Seasonal and diurnal variations of raindrop size distribution in Asian monsoon region. J Meteorol Soc Jpn. doi:10.2151/jmsj.84A.195

Maitra A (2000) Three-parameter raindrop size distribution modelling at a tropical location. Electron Lett. doi:10.1049/el:20000667

Maitra A, Das S, Shukla AK (2009) Joint statistics of rain rate and event duration for a tropical location in India. Indian Journal of Radio and Space Physics 38:253–260

Marshall JS, Palmer WM (1948) The distribution of rain drop with size. J Meteorol 5:165–166

Narayana Rao T, Narayana RD, Raghavan S (1999) Tropical precipitating systems observed with Indian MST radar. Radio Sci 5:1125–1139

Obiyemi OO, Ibiyemi TS, Ojo JS (2016) On validation of the rain climatic zone designations for Nigeria. Theor Appl Climatol. doi:10.1007/s00704-016-1787-9

Prat OP, Barros AP (2010) Ground observations to characterize the spatial gradients and vertical structure of orographic precipitation – experiments in the inner region of the great Smoky Mountains. J Hydrol 391(1–2):141–156

Rao TN, Rao DN, Mohan K, Raghavan S (2002) Classification of tropical precipitating systems and associated Z-R relationships. JGeophys Res 106:17,699–17,711

Sekhon RS, Srivastava RC (1971) Doppler radar observations of drop-size distributions in a thunderstorm. J AtmosSci 28:983–994

Short DA, Kozu T, Nakamura K (1990) Rainrate and raindrop size distribution observations in Darwin, Australia in proceedings of URSI commission F open symposium on regional factors in predicting Radiowave attenuation due to rain. Int. Union of Radio Sci. Comm, Rio de Janeiro, pp 35–40

Sivaramakrishnan MV (1961) Studies of raindrop size characteristics in different types of tropical rain using a simple raindrop recorder, Indian J. Meteorol Geophys 12:189–217

Tenório RS, Moraes MCDS, Sauvageot H (2012) Raindrop size distribution and radar parameters in coastal tropical rain systems of Northeastern Brazil. J Appl Meteorol Climatol 51:1960–1970

Testud J, Oury S, Blank RA, Amayenc P, Dou X (2001) The concept of "normalized" distribution to describe rain drop spectra: a tool for cloud physics and cloud remote sensing. J Appl Met 40:1118–1140

Thurai M, Bringi VN, May PT (2010) CPOL radar-derived drop size distribution statistics of stratiform and convective rain for two regimes in Darwin, Australia. J Atmos Ocean Technol 27:932–942. doi:10.1175/2010JTECHA1349.1

Timothy KI, Ong JT, Choo EBL (2002) Rain drop size distribution using method of moments for terrestrial and satellite communication applications in Singapore. IEEE Transaction on Antennas and Propagation 50(10):1420–1424

Tokay A, Short D (1996) Evidence from tropical rain drop spectra of the origin of rain from stratiform versus convective. J Appl Meteor 35:355–371

Ulbrich C (1983) Natural variations in the analytical form of the rain drop size distribution. J Clim And Appl Meteorol 22:1764–1775

Waldvogel A (1974) The N_0 jump of rain drop spectra. J Atmos Sci 31:1067–1078

Williams CR, Ecklund WL, Gage KS (1995) Classification of precipitating clouds in the tropics using 915 MHz wind profilers. Journal of Atmospheric Oceanic Technology 12:996–1012

Zawadski I, Monteiro E, Fabry F (1994) The development of drop size distributions in light rain. J Atm Sci 51:1100–1113